Available online at www.sciencedirect.com
SciVerse ScienceDirect
Acta Materialia 59 (2011) 7530–7537
Acta MATERIALIA
www.elsevier.com/locate/actamat

Ion irradiation of novel yttrium/ytterbium-based pyrochlores: The effect of disorder

Karl R. Whittle [a,*], Mark G. Blackford [a], Robert D. Aughterson [a], Gregory R. Lumpkin [a], Nestor J. Zaluzec [b]

[a] *Institute of Materials Engineering, ANSTO, PMB 1, Menai, NSW 2234, Australia*
[b] *Materials Science Division, Argonne National Laboratory, 9700 South Cass Avenue, IL 60439, USA*

Received 21 July 2011; received in revised form 9 September 2011; accepted 11 September 2011
Available online 15 October 2011

Abstract

Pyrochlores based on the general composition Ln_2TiO_5 ($Ln_{2.67}Ti_{1.33}O_{6.67}$) and $Ln_2Ti_2O_7$, where Ln = Y or Yb, have been irradiated through the crystalline–amorphous transition with 1 MeV Kr ions at the IVEM-TANDEM facility, Argonne National Laboratory. The results show that the T_c (critical temperature for amorphization) differs significantly between each series, e.g. for Y_2TiO_5 it is 589 ± 18 K and for $Y_2Ti_2O_7$ 665 ± 33 K. The difference suggests that recovery from damage is more rapid with increasing Ln content, i.e. a lower T_c for amorphization. These results are discussed in the context of the melting points of each phase, atomic disorder, the pyrochlore–fluorite order–disorder transition and the implications for oxide dispersion-strengthened additives.

Keywords: Radiation damage; Pyrochlore; Oxide dispersion strengthened

1. Introduction

The resistance of materials to radiation damage is a vital factor when determining the ideal materials for use as a waste form [1], a new fuel type, e.g. inert matrix fuels (IMF), or other applications within the nuclear fuel cycle. However, it is not always possible to undertake experiments using radioactive decay as the time-scales can make the studies complex, difficult and expensive. One method for accelerating the effect of damage is ion beam irradiation [2], allowing systems to be studied rapidly and systematically. Two factors directly effecting radiation stability are the roles crystal structure and chemical composition play, i.e. which is the major component determining stability/recovery from damage [2–4]. As part of this process we have studied materials closely related to pyrochlore but which differ in composition, i.e. A_2BO_5 as opposed to $A_2B_2O_7$. In this study we have prepared $Y_2Ti_2O_7$, Y_2TiO_5, $YbYTiO_5$, Yb_2TiO_5 and $Yb_2Ti_2O_7$ under identical conditions, subsequently irradiating them using the IVEM-TANDEM facility at Argonne National Laboratory.

The pyrochlore structure is well known, with many applications [5,6], examples of which include oxide fast ion conductors [7–12] and matrices for nuclear waste immobilization [2,13,14]. These applications are currently of major interest, as in both cases pyrochlores are capable of overcoming many technological problems while remaining cost effective. The ideal pyrochlore ($A_2B_2O_7$, $A = 2^+/3^+$, $B = 5^+/4^+$) structure can be described as a $2 \times 2 \times 2$ superstructure of fluorite (M_4X_8), with an ordered vacancy within the anion array. Such a vacancy allows the surrounding anions to relax from the ideal position in fluorite, giving rise to an observable superstructure in the anionic array. In conjunction with this relaxation the cations are ordered in chains, parallel to [1 1 0], with each cation species separated by (½ ½ ½), giving rise to an observable superstructure in the cation array. The addition of both superstructures changes the observed symmetry

---

[*] Corresponding author.
E-mail addresses: karlwhittle@me.com, karl.whittle@ansto.gov.au (K.R. Whittle).

1359-6454/$36.00
doi:10.1016/j.actamat.2011.09.021

from $Fm\bar{3}m$ to $Fd\bar{3}m$. This joint superstructure is visible using electron, X-ray or neutron diffraction and can be used to study the disordering processes within materials. An example structure is shown in Fig. 1a.

The general formulation $A_2B_2O_7$ is only one composition that can adopt the pyrochlore structure, with many containing vacancies [15] in A or B, e.g. AB_2O_6. Previously it has been reported that Ln_2TiO_5 ($Ln_{2.67}Ti_{1.33}O_{6.67}$) can adopt the pyrochlore structure for the majority of lanthanides (Gd–Lu) [16,17]. For lanthanides below Gd an orthorhombic structure is adopted, with atypical Ti–O and Ln–O coordination [18]. However, between Gd and Ho the cubic phase is a high temperature phase, whereas between Er and Lu it is stable under ambient conditions. In this type of pyrochlore there is intrinsic disorder across one of the two cation sites, in this case the B site, and extra vacancies within the anionic array, i.e. Y_2TiO_5 is $Y_2(Ti_{1.33}Y_{0.67})O_{6.67}$ (shown in Fig. 1b). A further, but equally valid, application of $Y_2Ti_2O_7$ and Y_2TiO_5 (where the material is expected to adopt the orthorhombic structure) is as an additive within oxide dispersion strengthened (ODS) steels [19,20], however, how the oxide behaves under conditions commensurate with a nuclear core is still not fully understood. These structures provide a mechanism by which the effects of disorder in pyrochlores/fluorites can be examined as a function of radiation tolerance, with a minimal change in composition.

2. Experimental

Samples were prepared by the calcination of metal oxides using stoichiometric amounts of Y_2O_3 (Aldrich, 99.9%), Yb_2O_3 (Aldrich, 99.9%) and TiO_2 (99.9%) which had previously been heated at 850 °C for 12 h to remove any absorbed H_2O/CO_2. The powders were ball milled to ensure complete mixing, pressed into pellets using cold isostatic pressing and heated at 1550 °C for 48 h, with heating and cooling rates of 5 K min^{-1}. Once cold the pellets were crushed to a fine powder using a mortar and pestle and analysed using powder X-ray diffraction (XRD) to ensure the samples were single phase. The diffraction data were collected with a Panalytical X'pert Pro and an Xcellerator PSD in the range $2\theta = 5$–80°, with an average step size of 0.01° and total count time of 100 s per point, with weighted Cu Kα radiation. The unit cell sizes were subsequently determined by Le Bail analysis [21] of the recorded patterns, using GSAS [22] and EXPGUI [23].

Selected area electron diffraction patterns were collected, prior to irradiation, using a JEOL 2010F transmission electron microscope, at an accelerating voltage of 200 keV. The samples were examined as crushed grains on holey carbon-coated Cu grids.

The samples were irradiated, again as crushed grains dispersed on a holey carbon-coated Cu grids, using the IVEM-TANDEM facility at the Argonne National Laboratory [24], with 1 MeV Kr^{2+} ions, in situ within a Hitachi 9000-NAR transmission electron microscope. A Gatan liquid helium (LHe) cooling stage was used for temperatures between 50 and 275 K, and a Gatan heating stage between room temperature and 650 K.

To minimize irradiation-induced temperature changes a fluence of 6.25×10^{11} ions $cm^{-2}\,s^{-1}$ was used, with the sample angled midway between the incident ion and electron beams, ~15° to the vertical. During irradiation the electron beam was switched off to prevent synergistic interactions of the electron and ion beams within the sample.

Multiple grains were irradiated simultaneously, with the point of amorphization being the point at which no Bragg diffraction intensities were visible in the selected area diffraction pattern. This is defined as the critical fluence (F_c) for the sample at the temperature of measurement. The data were subsequently analysed to determine the critical temperature (T_c), the temperature at which the rate of crystalline recovery is equal to the damage rate and above which the samples does not amorphize, under the same irradiation conditions. This temperature is determined by

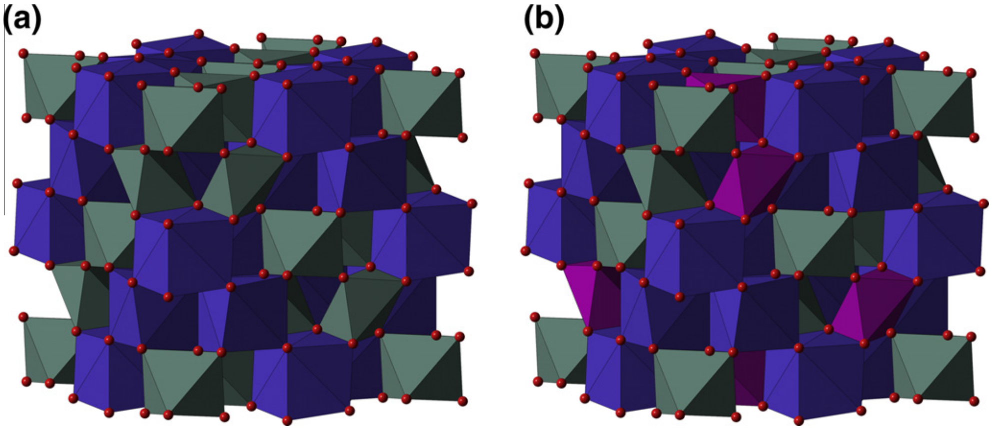

Fig. 1. Crystal structure representations of (a) $Ln_2Ti_2O_7$ and (b) $Ln_2Ti_{1.33}Ln_{0.67}O_{6.67}$ (Ln_2TiO_5). The changed colour in (b) is indicative of the replacement of Ti by Ln and does not represent the degree of ordering. (For interpretation of the references to colour in this figure legend, the reader is referred to the web version of this article.)